PROCEEDINGS OF SCIENCE

Recombination of heavy quarks for meson and baryon production in a large range of collisions systems

Vincenzo Minissale,[a,b,*] **Salvatore Plumari**[a,b] **and Vincenzo Greco**[a,b]

[a] *Department of Physics and Astronomy "E. Majorana", University of Catania, Via S. Sofia 64, 1-95123 Catania, Italy*

[b] *Laboratori Nazionali del Sud, INFN-LNS, Via S. Sofia 62, I-95123 Catania, Italy*

E-mail: vincenzo.minissale@dfa.unict.it

Measurements of heavy baryon production in pp, pA and AA collisions from RHIC to top LHC energies have recently attracted more and more attention, currently representing a challenge for the heavy-quark hadronization theoretical understanding. In such experiments there have been many indications of the formation of a deconfined phase of quarks and gluons called the quark-gluon-plasma (QGP). The large baryon over meson ratio $\Lambda_c/D^0 \sim O(1)$ observed in both AA collisions at RHIC and LHC as well as in pp collisions at 5.02 and 13 TeV has been well described by an hadronization approach based on the recombination of heavy quarks combined with fragmentation. The obtained ratio is, in general, quite larger than the one measured and expected in e^+e^-, ep collisions. The same approach also predicts a quite large $\Xi_c/D^0 \sim 0.15$ and $\Omega_c/D^0 \sim 0.05$ in pp collisions, in quite good agreement with experimental measurements. Given such successful predictions, we present here a critical assessment of the elements of the hadronization modeling that are mainly driving heavy baryon enhancement. In addition, we discuss the extensions of the approach applied in order to supply the prediction for the multi-charmed baryon production, i.e. Ξ_{cc}, Ω_{cc} and Ω_{ccc}, over a wide system size scan from $PbPb$ to $KrKr$, $ArAr$ and OO, and the bottomed hadron production in pp and $PbPb$ collisions. We can compare the coalescence prediction with the one coming from a statistical hadronization approach, investigating further the impact on the production coming from non-equilibrium features in the heavy-quark distribution that comes from the solution of relativistic Boltzmann or Langevin equation that describes the QGP evolution.

The European Physical Society Conference on High Energy Physics (EPS-HEP2025)
7-11 July 2025
Marseille, France

*Speaker

 ISSN 1824-8039 . Published by SISSA Medialab.

PoS(EPS-HEP2025)210

1. Introduction

Experimental data from RHIC and LHC have confirmed the formation of a quark-gluon plasma (QGP). Heavy quarks, such as charm and bottom, are produced in the early stages of the collision through well-understood mechanisms described by perturbative QCD. Due to their large mass, they experience the entire evolution of the QGP, making them excellent probes for studying the medium's properties. One particularly important aspect is their hadronization to form heavy hadrons like D and B mesons or Λ_c and Λ_b baryons. This process significantly influences key observables such as the transverse momentum spectra and the nuclear modification factor (R_{AA}), which provide insight into the nature of the medium and the interactions between heavy quarks and the QGP.

Measurements of $R_{AA}(p_T)$ and elliptic flow $v_2(p_T)$ for D mesons show that charm quarks lose energy in the QGP and participate in the collective motion of the medium [1–13]. Moreover, experimental results at LHC energies reveal an enhancement in the Λ_c/D^0 ratio in both PbPb and high-multiplicity pp collisions. This increase is driven by a Λ_c production much larger than predicted by fragmentation process, as shown by comparisons with fragmentation fractions measured in e^+e^- and ep collisions. These findings suggest that more complex hadronization mechanisms, such as coalescence combined with fragmentation, are relevant not only in heavy-ion collisions but also in smaller systems like pp collisions. Recent studies have demonstrated that such hybrid models qualitatively reproduce experimental data well [15–17]. Several theoretical models, both with and without recombination, have been proposed to explain these phenomena; a comprehensive comparison can be found in reference [14].

2. Coalescence plus fragmentation model

The coalescence mechanism was originally proposed as a hadronization model for heavy-ion collisions at RHIC, aiming to describe the transverse momentum spectra, baryon-to-meson ratios, and the observed splitting in elliptic flow between mesons and baryons [18, 19]. This approach was later successfully applied at LHC energies, providing a consistent description of light hadron spectra and baryon-to-meson ratios [20]. Subsequently, it was extended to the hadronization of heavy-flavor quarks in nucleus-nucleus (AA) collisions [21–24], and more recently to the production of multi-charmed hadrons such as Ξ_{cc} and Ω_{ccc} [25]. The recombination model employed in this work is based on the Wigner formalism. The hadron spectrum as a function of transverse momentum formed by coalescence of quarks can be written as:

$$\frac{dN_H}{dyd^2P_T} = g_H \int \prod_{i=1}^{N_q} \frac{d^3p_i}{(2\pi)^3 E_i} p_i \cdot d\sigma_i \; f_{q_i}(x_i, p_i) C_H(x_1 ... x_{N_q}, p_1 ... p_{N_q}) \, \delta^{(2)} \left(P - \sum_{i=1}^{n} p_i \right)$$

Where g_H represents the combinatorial factor to form a colorless hadron from quarks and antiquarks with spin 1/2. $d\sigma_i$ refers to an element of a space-like hypersurface at a fixed proper time τ that corresponds to the QGP lifetime, while f_{q_i} denotes the quark (anti-quark) phase-space distribution functions for the i-th quark (anti-quark). The function $C_H(x_1 ... x_{N_q}) = C^{N_q - 1} f_H(x_1 ... x_{N_q}, p_1 ... p_{N_q})$ is expressed in terms of the Wigner function $f_H(x_1 ... x_{N_q}, p_1 ... p_{N_q})$ that describes the spatial and momentum distribution of quarks in a hadron, and the factor $C^{N_q - 1}$ which is fixed to impose that the total coalescence probability gives $\lim_{p \to 0} P^{tot}_{coal} = 1$. The Wigner function assumed here is

a Gaussian in both position and momentum space, i.e. $f_H(...) = \prod_{i=1}^{N_q-1} 8 \exp\left(-\frac{xri^2}{\sigma_{ri}^2} - p_{ri}^2\sigma_{ri}^2\right)$, where x_{ri} and p_{ri} represent the relative coordinates. The widths σ_{ri} are connected to the the root mean square charge radius of the hadron produced, for details see refs.[15, 22, 25, 26]. Previous investigations of heavy-quark (HQ) recombination [4, 20–22, 27] have consistently shown that the coalescence probability decreases with increasing transverse momentum (p_T). This trend implies that, at high p_T, hadron formation is predominantly governed by independent fragmentation rather than recombination. To model a continuous transition between the low and high p_T regimes, we introduce a momentum-dependent fragmentation probability, $P_{\rm frag}(p_T)$. In this framework, heavy quarks with finite transverse momentum hadronize either through coalescence or fragmentation, with the respective probabilities given by $P_{\rm coal}(p_T)$ and its complement $P_{\rm frag} = 1 - P_{\rm coal}$. For the fragmentation process, we adopt the Peterson fragmentation function for charm hadrons [28] and the Kartvelishvili parametrization for bottom hadrons [29].

3. Hadron production for single and multi-charmed particles, from pp to AA collisions

The combined hadronization mechanism of heavy quarks through coalescence and fragmentation in AA collisions at RHIC and LHC energies leads to a pronounced enhancement in baryon production. In particular, Λ_c yields are significantly increased at low transverse momentum ($p_T \lesssim$ 3–4 GeV), resulting in a characteristic rise-and-fall trend in the heavy-flavor baryon-to-meson ratio [21, 22]. For pp collisions, under the assumption of a QGP-like medium formation [31, 32], the model predictions for D^0, D^+, D^*, and Λ_c [15] are broadly consistent with those obtained from the Statistical Hadronization Model incorporating an extended baryon spectrum [33]. However,

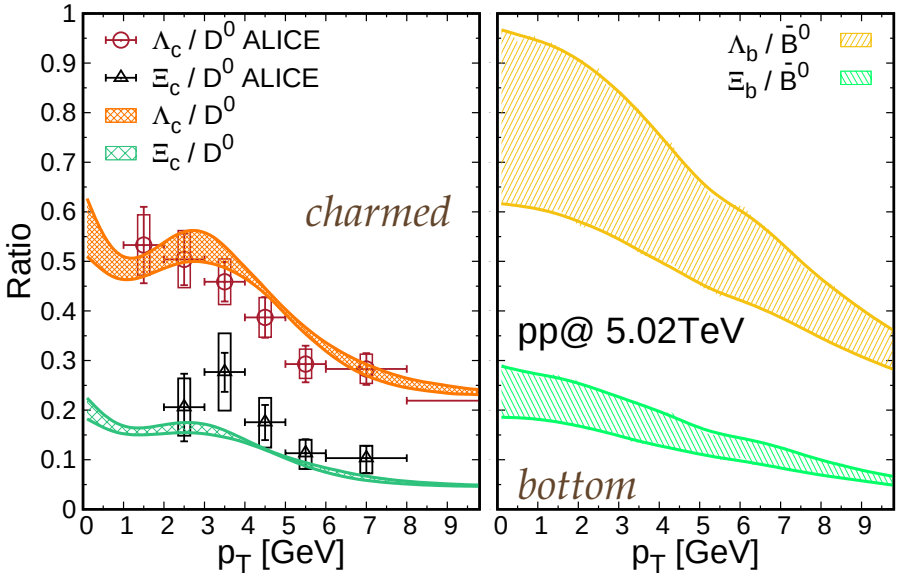

Figure 1: Baryon-to-meson ratios as a function of transverse momentum for pp collisions at $\sqrt{s}$ = 5.02 TeV: (left) Λ_c/D^0, Ξ_c/D^0 and (right) Λ_b/B^0, Ξ_b/B^0. The shaded bands represent variations in the Wigner width. Experimental data are taken from [34, 35].

substantial differences emerge for multi-strange charmed baryons such as Ξ_c and Ω_c. As shown in Fig. 1 (left panel), the coalescence-plus-fragmentation approach reproduces the charmed baryon-to-meson ratios observed in recent LHC measurements for pp collisions [34, 35]. The right panel of Fig. 1 displays the corresponding ratios for bottom baryons, $\Lambda_b/\bar{B^0}$ and $\Xi_b^0/\bar{B^0}$, in pp collisions at $\sqrt{s}$ = 5.02 TeV. The hybrid model predicts a stronger baryon enhancement in the bottom sector compared to charm. Specifically, the Λ_b/B^0 ratio reaches approximately 0.9 at low p_T, about 50% higher than the charmed counterpart, while maintaining a decreasing trend at larger p_T. For $\Xi_b^0/\bar{B^0}$, the ratio is around 0.3 at low momenta, roughly 30% smaller than $\Lambda_b/\bar{B^0}$, reflecting a pattern similar to that observed between Λ_c and Ξ_c in the charm sector.

We extended our analysis of charmed and multi-charmed hadron production in AA collisions by exploring systems of different sizes, including *PbPb*, *KrKr*, *ArAr*, and *OO*. Figure 2 shows the yields for the main single and multi-charmed hadrons in AA collisions at mid-rapidity for 0–10% centrality. The error bands indicate the range of the predicted yields: the lower bound corresponds to a realistic charm-quark distribution, while the upper bound assumes full thermalization. While the choice of distribution has little impact on D^0 and Λ_c production, it strongly affects multi-charmed baryons, whose yields increase substantially under thermalized conditions. This trend reflects the fact that thermalization enhances the population of low-momentum charm quarks, favoring recombination and thus boosting multi-charmed baryon formation. The observed sensitivity of these yields confirms the expectation that multi-charmed baryons are more dependent on the underlying charm distribution than single-charmed hadrons. Figure 2 compares production across different collision systems *PbPb*,*KrKr*, *ArAr*, and *OO*. For these systems, the initial p_T spectra are obtained

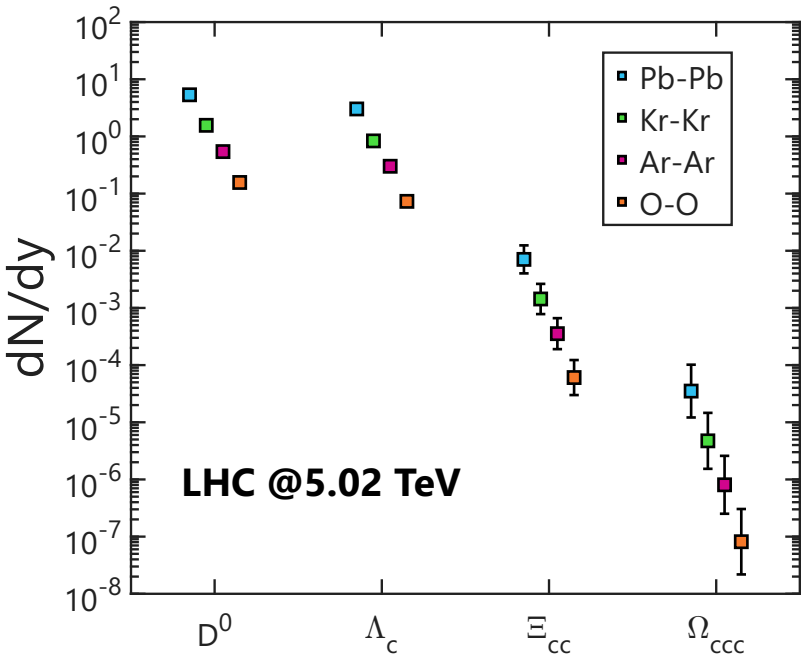

Figure 2: Mid-rapidity dN/dy for single- and multi-charmed hadrons in various collision systems, calculated using the coalescence-plus-fragmentation approach. Error bands indicate the yield range, where the lower bound corresponds to a realistic charm-quark distribution and the upper bound assumes full thermalization.

from FONLL calculations and evolved in a QGP medium using a relativistic Boltzmann transport approach, as detailed in [25]. A key difference arising from system size is that smaller systems have shorter lifetimes and reduced QGP exposure, leading to less energy loss and consequently flatter final p_T distributions compared to larger systems [25]. A comparison with Statistical Hadronization Model predictions and a discussion of expected scaling with system size can be found in [25].

References

[1] P.B. Gossiaux, J. Aichelin, Phys. Rev. C **78**, 014904 (2008).

[2] M. He, R.J. Fries, R. Rapp, Phys. Rev. Lett. **110**, 112301 (2013).

[3] J. Uphoff, O. Fochler, Z. Xu, C. Greiner, Phys. Lett. **B717**, 430 (2012).

[4] S. Cao, G.Y. Qin, S.A. Bass, Phys. Rev. **C92**, 024907 (2015).

[5] A. Beraudo, A. De Pace, M. Monteno, M. Nardi, F. Prino, JHEP **05**, 279 (2021).

[6] M.L. Sambataro, Y. Sun, V. Minissale, S. Plumari, V. Greco, Eur. Phys. J. C **82**, 833 (2022).

[7] M.L. Sambataro, V. Minissale, S. Plumari, V. Greco, Phys. Lett. B **849**, 138480 (2024).

[8] M. L. Sambataro, V. Minissale, S. Plumari and V. Greco, arXiv:2508.01024.

[9] S. Plumari, G.L. Guardo, F. Scardina, V. Greco, Phys. Rev. **C92**, 054902 (2015).

[10] F. Scardina, S.K. Das, V. Minissale, S. Plumari, V. Greco, Phys. Rev. **C96**, 044905 (2017).

[11] S. Plumari, G. Coci, V. Minissale, S.K. Das, Y. Sun, V. Greco, Phys. Lett. B **805**, 135460 (2020).

[12] Y. Sun, S. Plumari, V. Greco, Eur. Phys. J. C **80**, 16 (2020).

[13] L. Oliva, S. Plumari, V. Greco, JHEP **05**, 034 (2021).

[14] J. Zhao, J. Aichelin, P. B. Gossiaux, A. Beraudo, S. Cao, W. Fan, M. He, V. Minissale, T. Song and I. Vitev, *et al.* Phys. Rev. C **109** (2024) no.5, 054912

[15] V. Minissale, S. Plumari, V. Greco, Phys. Lett. B **821**, 136622 (2021).

[16] A. Beraudo, A. De Pace, D. Pablos, F. Prino, M. Monteno, M. Nardi, Phys. Rev. D **109**, L011501 (2024).

[17] J. Zhao, J. Aichelin, P.B. Gossiaux, K. Werner, Phys. Rev. D **109**, 054011 (2024).

[18] V. Greco, C. Ko, P. Levai, Phys.Rev.Lett. **90**, 202302 (2003).

[19] R. Fries, B. Muller, C. Nonaka, S. Bass, Phys. Rev. Lett. **90**, 202303 (2003).

[20] V. Minissale, F. Scardina, V. Greco, Phys. Rev. C **92**, 054904 (2015), 1502.06213.

[21] Y. Oh, C.M. Ko, S.H. Lee, S. Yasui, Phys. Rev. C **79**, 044905 (2009), 0901.1382.

[22] S. Plumari, V. Minissale, S.K. Das, G. Coci, V. Greco, Eur. Phys. J. **C78**, 348 (2018).

[23] S. Cho, K.J. Sun, C.M. Ko, S.H. Lee, Y. Oh, Phys. Rev. C **101**, 024909 (2020).

[24] M. He, R. Rapp, Phys. Rev. Lett. **124**, 042301 (2020), 1905.09216.

[25] V. Minissale, S. Plumari, Y. Sun, V. Greco, Eur. Phys. J. C **84**, 228 (2024), 2305.03687.

[26] V. Minissale, V. Greco and S. Plumari, Phys. Lett. B **860** (2025), 139190

[27] P.B. Gossiaux, R. Bierkandt, J. Aichelin, Phys. Rev. C **79**, 044906 (2009), 0901.0946.

[28] C. Peterson, D. Schlatter, I. Schmitt, P.M. Zerwas, Phys. Rev. **D27**, 105 (1983).

[29] V.G. Kartvelishvili, A.K. Likhoded, V.A. Petrov, Phys. Lett. B **78**, 615 (1978).

[30] A. Andronic, et al. JHEP **07**, 035 (2021).

[31] R.D. Weller, P. Romatschke, Phys. Lett. B **774**, 351 (2017), 1701.07145.

[32] M. Greif, C. Greiner, B. Schenke, S. Schlichting, Z. Xu, Phys. Rev. D **96**, 091504 (2017).

[33] M. He, R. Rapp, Phys. Lett. B **795**, 117 (2019).

[34] S. Acharya et al. (ALICE), Phys. Rev. C **104**, 054905 (2021), 2011.06079.

[35] S. Acharya *et al.* [ALICE], JHEP **10** (2021), 159 doi:10.1007/JHEP10(2021)159